



Effect of Grain Disorientation on Early Fatigue Crack Propagation in FCC Polycrystals: Dislocation Dynamics Simulations and Corresponding Experimental Validation

Christian Robertson, G V Prasad Reddy, Christophe Déprés, Marc C. Fivel

► To cite this version:

Christian Robertson, G V Prasad Reddy, Christophe Déprés, Marc C. Fivel. Effect of Grain Disorientation on Early Fatigue Crack Propagation in FCC Polycrystals: Dislocation Dynamics Simulations and Corresponding Experimental Validation. 7th International conference on Creep, Fatigue and Creep-Fatigue interaction (CF7), Jan 2016, Kalpakkam, India. pp.477-481, 10.1007/s12666-015-0754-y . hal-01459847

HAL Id: hal-01459847

<https://hal.science/hal-01459847>

Submitted on 7 Feb 2017

HAL is a multi-disciplinary open access archive for the deposit and dissemination of scientific research documents, whether they are published or not. The documents may come from teaching and research institutions in France or abroad, or from public or private research centers.

L'archive ouverte pluridisciplinaire **HAL**, est destinée au dépôt et à la diffusion de documents scientifiques de niveau recherche, publiés ou non, émanant des établissements d'enseignement et de recherche français ou étrangers, des laboratoires publics ou privés.

Effect of grain disorientation on early fatigue crack propagation in FCC polycrystals: dislocation dynamics simulations and corresponding experimental validation

C. Robertson^c, G.V.PrasadReddy^{a,b}, C. Déprés^a, M.Fivel^d

^aLaboratory SYMME, Université de Savoie, BP80439, 74944 Annecy-le-Vieux Cedex, France

^bIndira Gandhi Centre for Atomic Research, Kalpakkam, Tamil Nadu 603102 INDIA

^cCEA, DEN, Service de Recherche Métallurgiques Appliquées, F91191 Gif-sur-Yvette, France

^dSIMaP-GPM2, Grenoble INP, CNRS/UJF, 101 Rue de la Physique, BP 46, 38402 St Martin d'Hères cedex, France

Abstract

3-dimensional dislocation dynamics (DD) simulations are performed, in face-centred cubic bi-crystals, to study the microcrack interaction with first microstructural barrier under high cycle fatigue (HCF) loading conditions. Based on experimental observations, we presumed that microcracks are blocked by grain boundaries and that subsequent propagation/transmission occurs by the growth of surface relief in a secondary grain adjoining the primary crack. This mechanism is herein called *indirect transmission* and is found to strongly depend on grain-to-grain disorientation. A semi-analytical model proposed earlier is discussed with the DD simulation results in the context of first-barrier compliance. The proposed model describes the documented experimental results related to the effect of grain size, grain misorientation and microcrack propagation kinetics in fatigued 316L steel polycrystals.

1.0 Introduction

In face-centered cubic (FCC) single-phase polycrystals, with no defects and/or precipitates, the initiation of stage-I fatigue cracks usually occurs in the surface grains. Prior to the microcrack initiation, significant surface markings develop in the form of extrusions concomitant with the formation of persistent slip bands (PSBs) that form the basis for the nucleation of microcracks [1-3]. In subsequent to the microcrack initiation, microcrack propagates until it encounters the first microstructural barrier (*i.e.* a grain boundary). As a result, the subsequent crack propagation or retardation not only depends strongly on the loading amplitude, but also on the next (or secondary) grain orientation [4] defined by the tilt, twist and theta angles (as per refs. [5,6]).

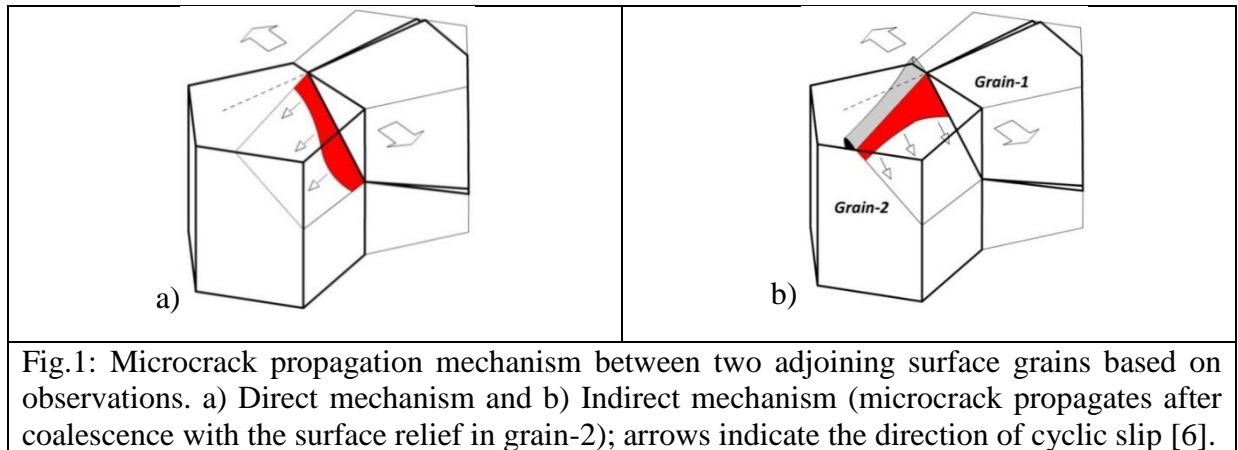


Fig.1: Microcrack propagation mechanism between two adjoining surface grains based on observations. a) Direct mechanism and b) Indirect mechanism (microcrack propagates after coalescence with the surface relief in grain-2); arrows indicate the direction of cyclic slip [6].

This paper briefly presents a micro-mechanical model and its application in terms of microcrack growth prediction, and also its validation with the experimental results, in the context of the experimentally observed *indirect transmission mechanism*. Therefore, our simulations do not apply to prior or subsequent crack development stages and therefore substantially differ from all the previous crack-tip plasticity investigations [7-9].

2.0 Dislocation dynamics simulation setup

2.1 Simulation geometry and parameters

The DD-code used for this study is an edge-screw model called TRIDIS, developed at SIMaP laboratory [11]. The material parameters used for austenitic stainless steel are given elsewhere [6]. The implementation of thermally-activated cross-slip is done as per the explanation in [12,13]. A pseudo bi-crystal aggregate simulation setup (Fig.1b) is considered to investigate the indirect crack transmission mechanism. In Fig.1b, *grain-1* is denoted as primary grain and it includes an arrested crack and no dislocations. It is important to mention that grain-1 geometry can be chosen arbitrarily and has no effect on this study. The pentagonal shape shown in Fig.1 is adopted for simplicity. The DD simulations are carried out in secondary grain (i.e. *grain-2*) and both grains are defined as 5-faceted cylinders. The grain axis is aligned perpendicularly to the grain free surface (see Fig.1). Dislocations gliding in grain-2 can escape through the top surface of simulated volume, whereas all the other surfaces act as strong and impenetrable obstacles. Each dislocation segment leaving the crystal through the top boundary produces a step in the corresponding surface [14]. Image forces are not implemented in our simulations, since their influence on PSB slip activity is noticed to be negligible [15], even in the presence of a crack [16]. The initial, grain-2 dislocation microstructure consists of 24 Frank-Read sources, 2-sources on each of the 12 FCC slip systems $a/2\langle 110 \rangle \{111\}$. The sources are simply placed (inside grain-2) within 1 μm of the arrested crack tip and evolve according to the local, effective stress conditions (including the primary crack stress field). The DD simulations are carried out with a fully reversed cyclic strain for applied plastic strain ranges of $\Delta\varepsilon_p = 10^{-4}$ and 2×10^{-4} compatible with HCF conditions. The applied stress level is monitored and controlled as detailed in [14]. All the simulations are performed under isothermal conditions at 300K.

2.2 Implementation of heterogeneous crack stress field

The microcrack in the grain-1 induces a long-range stress field in the surrounding elastic medium comprising grain-2. The effect of crack stress field is treated using the superimposition principle where the total stress applied to each dislocation segment (within grain-2) is taken as the sum of: (i) applied stress (homogeneous stress), (ii) the dislocation-induced stress (internal stress), and (iii) the crack stress field (heterogeneous stress), calculated using Eqs.1-4 from reference [6]. DD simulations were performed for varying orientations of the grain-2, with respect to the crack plane. The simulation results are analysed by means of a semi-quantitative model, to be presented in the next section.

3.0 Discussion: DD simulation based microcrack transmission model

In response to the applied stress, the mobile dislocations introduced (in grain-2) near the crack front zone glide into several different parallel planes and gradually develop pile-ups at the grain boundary. It is possible to calculate the stress-strain response associated with the

dislocation structures in crack tip region, by considering \mathcal{N} slip planes¹ for which the simplified analytical solution is [6]:

$$\Delta \tau_{local,wc} = \frac{1}{\mathcal{N}} \left[\frac{1}{S} \frac{\mu}{(1-\nu)} \right] \Delta \gamma_{local,wc} \quad (1)$$

where $\Delta \gamma_{local,wc}$ and $\Delta \tau_{local,wc}$ are the shear strain and shear stress ranges acting in the crack tip region (the subscript implies: "local, with crack"), μ the shear modulus, ν the Poisson ratio and S is a dimensionless parameter characterizing the grain geometry [15,17]. To derive the 'microcrack transmission semi-analytical model', the different terms in Eq.1 will be evaluated separately, as explained in next two paragraphs.

Evaluation of $\Delta \tau_{local,wc}$: The shear stress range in the crack tip region is given by:

$$\Delta \tau_{local,wc} \approx \frac{\Delta K_0}{\sqrt{2\pi r}} = \Delta \tau_{global,wc}^* \sqrt{\frac{\pi a}{2\pi r}} \quad (2)$$

where $\Delta \tau_{global,wc}^*$ is shear stress accumulated beyond the yield point, at the individual grain scale (and thus the subscript "global"). By equating the crack size $a \sim D_g$, on the presumption of fully cracked primary grain-1, one obtains:

$$\Delta \tau_{local,wc} \approx \Delta \tau_{global,wc}^* \sqrt{\frac{D_g}{2r}} \quad (3)$$

Evaluation of $\Delta \gamma_{local,wc}$: In the absence of a mean strain, surface displacement due to cyclic strain accumulation is given by [14]:

$$\gamma^{surf} \propto \eta \Delta \gamma_p \sqrt{N} \quad (4)$$

where $\Delta \gamma_p$ is the imposed plastic shear-strain range, N the cycle number and η is a dimensionless factor depending on simulation-setup and material parameters (see ref. [14] for the derivation of Eq.4 using DD simulations). On the other hand, in the presence of a mean strain (compression \neq tension), the accumulation of cyclic surface displacement is given by:

$$\gamma^{surf} \propto \eta \Delta \varepsilon_p \left(1 + 2 \frac{\bar{\gamma}_p}{\Delta \gamma_p} \right) \sqrt{N} \quad (5)$$

The Eq.5 is derived based on a series of cyclic simulations, where the level of mean strain $\bar{\gamma}_p$ is systematically changed, and the corresponding results plus physical interpretation were given in reference [18]. However, in the present study, to evaluate the quantity $\bar{\gamma}_p$ due to the primary crack, two separate DD simulations using a fixed plastic strain range $\Delta \gamma_p$ were performed. Firstly, a simulation is carried out without the influence of crack stress field (i.e. no crack) and generated a reference $\gamma_{woc}^{surf}(N)$ curve. This curve is then fitted with Eq.4, which is then subsequently solved to obtain a fixed η value. The second simulation is performed in the presence of a crack in grain-1 and the results are used to generate a $\gamma_{wc}^{surf}(N)$ curve. This new curve is then fitted using Eq.5, and it is assumed that the differences between γ_{wc}^{surf} and γ_{woc}^{surf} are due to the mean strain $\bar{\gamma}_p$ acting in the crack tip region. The obtained $\bar{\gamma}_p$ value is then finally inserted in Eq.1, assuming that $\Delta \gamma_{local,wc} = \bar{\gamma}_p$.

¹ The number of active slip planes \mathcal{N} must not be confused with the number of cycles N .

Inserting Eq.3 in the left-hand term of Eq.1 and rearranging the different terms gives:

$$\frac{D_g}{(2r)} = \left(\frac{1}{N} \left[\frac{1}{S} \frac{\mu}{(1-\nu)} \right] \frac{\Delta\gamma_{local,wc}}{\Delta\tau_{global,wc}^*} \right)^2 \quad (6)$$

Eq.6 is applied to various DD simulations conducted using varying twist angles for a fixed cyclic loading level $\Delta\gamma_p = 10^{-4}$. Each grain disorientation case gives: i) a given $\Delta\gamma_{local,wc}/\Delta\tau_{global,wc}^*$ ratio, to be called the *first-barrier compliance* and ii) a specific curve in Fig.2a. In general, microcrack transmission is a local process and takes place at the scale of individual shear bands in polycrystals [14]. Therefore, the surface displacements developed by individual shear bands need to be calculated in order to evaluate the microcrack transmission kinetics based on the *indirect mechanism*. From the above mentioned Eq.4 and Eq.5, the evolution of surface displacement in the whole crack tip zone is characterized by:

$$\frac{\gamma_{wc}^{surf}}{\gamma_{woc}^{surf}} = \left(1 + 2 \frac{\gamma_p}{\Delta\gamma_p} \right) \quad (7)$$

The surface displacement generated by a single shear band can be obtained by the ratio of right-hand term of Eq. 7 to the total number of active shear-bands N . The latter can be obtained by solving Eq.6, yielding:

$$\frac{\gamma_{wc}^{surf}}{\gamma_{woc}^{surf}} = \frac{\sqrt{\frac{D_g}{2r}}}{\left[\frac{1}{S} \frac{\mu}{(1-\nu)} \right] \left(\frac{\Delta\gamma_{local,wc}}{\Delta\tau_{global,wc}^*} \right)} \left(1 + \sqrt{\frac{D_g}{2r}} \right) \quad (8)$$

Eq.8 thus describes the accumulation of average surface displacement by single shear bands in grain-2, ahead of the primary crack front.

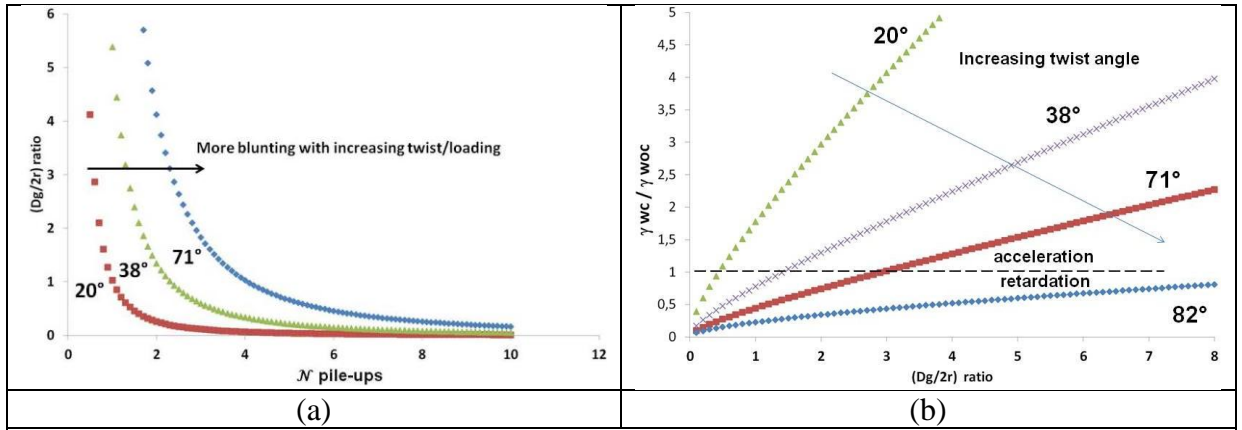


Fig.2: Model results. (a) Variation of parameter $(D_g/2r)$ i.e. reciprocal half-distance to the crack tip) as a function of 'number of active pile-ups N in the crack process zone'; increase in twist angle increases the plastic zone size. (b) Microcrack transmission kinetics towards the secondary grain as a function of twist angle; the results are normalized w.r.to the non-cracked case. A slip ratio of $\gamma_{wc}^{surf}/\gamma_{woc}^{surf} > 1$ means extrusion growth acceleration and < 1 implies extrusion growth retardation in the presence of crack. Twist angles = 20°, 38°, 71° and 82° are used for the same tilt-angle at $24^\circ \pm 2^\circ$ [6].

Eq.8 expression helps in analysing the simulation results and also in making direct comparisons between the simulation and experiment. For instance, its predictions are compared with microcrack kinetics observed in actual polycrystals, where the crystallographic

orientations of primary and secondary grains (and corresponding twist angle) are evaluated using electron back-scattering diffraction technique.

The crack initiation time N_{A2} and the crack arrest time $T_{1>2}$ are evaluated by observation of replicas extracted at different number of cycles. A correlation/equivalence can be drawn between the Fig.2 and Fig.3. Fig.2 indicates that plasticity spreading onto multiple slip bands increase with the twist angle, leading to less net surface relief. This in turn implies an increase in crack arrest time at primary grain boundary and also a simultaneous increase in crack initiation time, in the secondary grain. This can be seen from Fig.3 wherein large twist angles corresponding to low $1/\sqrt{T_{1>2}/N_{A2}}$ values denote a delay in crack transmission kinetics and conversely, at small twist angles.

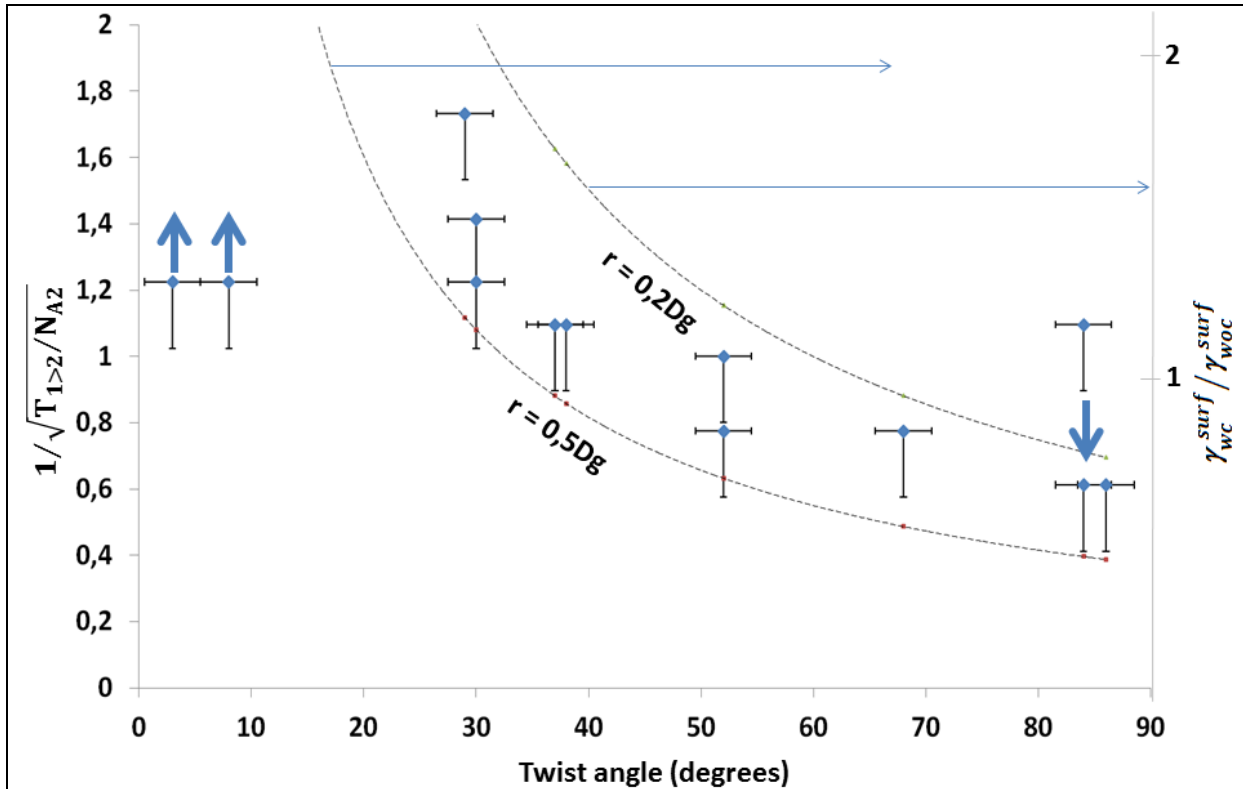


Fig.3: Microcrack propagation kinetics from primary to secondary grain: effect of twist angle. The micro-mechanic model predictions (dashed curves plotted for different distances r with respect to the primary crack tip region: $r = 0.2D_g$ and $r = 0.5D_g$ where D_g is the grain diameter) are directly compared with experimental observations. More specifically, $\gamma_{wc}^{surf}/\gamma_{woc}^{surf}$ ratio calculated using Eq.8 is directly compared to the $1/\sqrt{T_{1>2}/N_{A2}}$ quantity. The above two quantities are equivalent based on Eq.4 and Eq.5 and [14]; assuming that microcrack initiation takes place whenever γ_{wc}^{surf} or γ_{woc}^{surf} achieve a critical value, depending on the material, temperature and environmental conditions.

4.0 Conclusions/Summary

3-dimensional DD simulations performed in FCC bi-crystals to study the microcrack interaction with first microstructural barrier, under high cycle fatigue (HCF) loading conditions, provided interesting results. At first, DD simulations revealed that a cyclic slip localization or dispersion onto several slip bands is found to strongly depend on the twist angle. Our semi-analytical model developed based on the cyclic plasticity ahead of the crack

front is able to capture the above cyclic slip distribution. The model also predicts that an increase in twist angle (for a given $D_g/2r$ ratio) increases the development of active slip planes \mathcal{N} in the crack process zone. The DD simulation results fairly show equivalence with the results of crack initiation/arrest times obtained from actual experiments.

5.0 Acknowledgements

The authors acknowledge the financial support of the French National Agency for Research Agency through the AFGRAP project.

6.0 References

- [1] Basinski Z S, and Basinski S, J Prog Mater Sci 36 (1992) 89.
- [2] Man J, Obrtlik K, Blochwitz C and Polak J, Acta Mater 50 (2002) 3767.
- [3] Man J, Obrtlik K and Polak J, Phil Mag A 89 (2009) 1295.
- [4] Christ H J, Duber O, Fritzen C P, Knobbe H, Köster P, Krupp U, and Künkler B, Comput Mater Sci 46 (2009) 561.
- [5] Zhai T, Wilkinson A J and Martin J W, Acta Mater 48 (2000) 4917.
- [6] Prasad Reddy G V, Robertson C, Déprés C and Fivel M, Acta Mater 61 (2013) 5300.
- [7] Hansson P. Int J Fatigue 31 (2009) 1346.
- [8] Deshpande V S, Needleman A and Van der Giessen E, Acta Mater 51 (2003) 4637.
- [8] Van der Giessen E, Deshpande V S, Cleveringa H H M, and Needleman A J, Mechanics and Physics of Solids, 49 (2001) 2133.
- [10] Espinosa H D, Panico M, Berbenni S and Schwarz K W, Int J Plasticity 22 (2006) 2091.
- [11] Verdier M, Fivel M and Groma I, Mod Sim Mater SciEng 6 (1998) 755.
- [12] Déprés C, Robertson C, and Fivel M, Phil Mag A 84 (2004) 2257.
- [13] Robertson C, Fivel M, and Fissolo A, Mat SciEng A 315 (2001) 47.
- [14] Déprés C, Robertson C, and Fivel M, Phil Mag A 86 (2006) 79.
- [15] Déprés C, Modélisation physique des stades précurseurs de l'endommagement en fatigue dans l'acier inoxydable 316L, Doctoral Thesis, Institut National Polytechnique de Grenoble, France, 2004.
- [16] Déprés C, Prasad Reddy G V, Robertson C, and Fivel M, Phil Mag A 94 (2014) 4115.
- [17] Hirth J P, and Lothe J. Theory of Dislocations, McGraw-Hill (1982) p 770
- [18] Robertson C, Déprés C, and Fivel M, Special Issue of Trans. Indian Institute of Metals, 63 (2010) 529.